

Excitonic pairing of two-dimensional Dirac fermions near the antiferromagnetic quantum critical point

Hai-Xiao Xiao,¹ Jing-Rong Wang,² Zheng-Wei Wu,¹ and Guo-Zhu Liu^{1,*}

¹*Department of Modern Physics, University of Science and Technology of China, Hefei, Anhui 230026, P. R. China*

²*Anhui Province Key Laboratory of Condensed Matter Physics at Extreme Conditions, High Magnetic Field Laboratory of the Chinese Academy of Science, Hefei, Anhui 230031, P. R. China*

Two-dimensional Dirac fermions are subjected to two types of interaction, namely the long-range Coulomb interaction and the short-range on-site interaction. The former induces excitonic pairing if its strength α is larger than some critical value α_c , whereas the latter drives an antiferromagnetic Mott transition when its strength U exceeds a threshold U_c . Here, we study the impact of the interplay of these two interactions on the fate of excitonic pairing by using the Dyson-Schwinger equation approach. We find that the value of α_c is slightly increased by weak on-site interaction. As U grows to approach U_c , the quantum fluctuation of antiferromagnetic order parameter becomes important and interacts with Dirac fermions via the Yukawa coupling. After treating the Coulomb interaction and Yukawa coupling on equal footing, we show that α_c increases substantially as $U \rightarrow U_c$. Therefore, excitonic pairing is strongly suppressed near the antiferromagnetic quantum critical point. We obtain a global phase diagram on the U - α plane, and illustrate that the excitonic insulating and antiferromagnetic phases are separated by the gapless semimetal phase. These results provide a possible explanation of the discrepancy between recent theoretical progress on excitonic gap generation and existing experiments in suspended graphene.

I. INTRODUCTION

Two-dimensional (2D) massless Dirac fermions are the low-energy excitations of a number of condensed matter systems. Examples include d -wave high- T_c cuprate superconductors [1, 2], graphene [3–7], surface of three-dimensional (3D) topological insulators [8], and organic conductor α -(BEDT-TTF)₂I₃ [9]. While the single particle properties of Dirac fermion systems have already been extensively studied, the strong correlation effects are still not well understood. Ordinary metals are known to be robust against repulsive interactions [10], which renders the validity of Fermi liquid theory. In contrast, the repulsive interactions are much more important in 2D Dirac fermion systems, and may lead to several possible phase-transition instabilities [5–7]. Generically, there are two types of repulsive interactions, namely long-range Coulomb interaction and Hubbard-like on-site interaction. The former is spin blinded, whereas the latter acts on two electrons with different spins.

When the strength parameter U of on-site repulsive interaction is greater than a critical value U_c , there is a quantum phase transition from gapless semimetal (SM) to antiferromagnetic (AFM) Mott insulator [11]. The SM-AFM quantum critical point (QCP) falls in the universality class of Gross-Neveu-Yukawa model [11]. Apart from SM-AFM transition, Sato *et al.* [12] studied the transition between SM and Kekulé valence-bond solid caused by on-site interaction. When other sorts of repulsion are considered, SM materials could exhibit even richer phase-transition structures [12–19]. For instance, Raghu *et al.* [13] investigated the cooperative effects

of nearest-neighboring and next-neighboring repulsions within the mean-field approximation, and found a number of insulating phases, including charge density wave (CDW), AFM, and topological Mott phases that display quantum anomalous Hall (QAH) and quantum spin Hall (QSH) effects, although subsequent studies revealed that the topological Mott phases can be destroyed by fluctuations [16].

In case the Fermi level is located exactly at the band-touching point, the long-range Coulomb interaction is poorly screened due to the vanishing of density of states (DOS). If the Coulomb interaction is weak, the system remains gapless, but the fermion velocity is substantially renormalized [7, 20]. When the Coulomb interaction strength parameter α exceeds a critical value α_c , a finite energy gap is dynamically generated via the formation of excitonic-type particle-hole pairs [21–45]. This then turns the originally gapless SM into a gapped excitonic insulator (EI).

In previous works, the Coulomb interaction and the on-site interaction were usually investigated separately. Their interplay can give rise to some salient properties, especially in the strong coupling regimes. Interesting progress has recently been made towards more detailed knowledge of this interplay. Tang *et al.* [17] studied the influence of long-range Coulomb and on-site interactions on the ground-state properties of 2D Dirac fermion systems by combining the non-perturbative quantum Monte Carlo (QMC) simulation and the renormalization group (RG) technique. Their works [17] reproduced the previously discovered logarithmic velocity renormalization and also the SM-AFM transition at some critical value U_c . They further showed that U_c increases as α grows, which indicates that the Coulomb interaction disfavors AFM transition. These results are summarized in the phase diagram given by Figure 1 of Ref. [17].

*gzliu@ustc.edu.cn

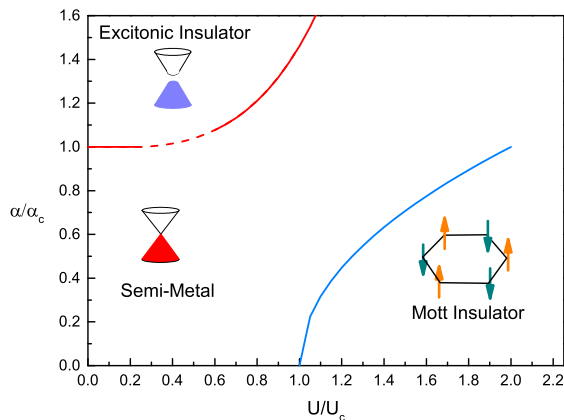


FIG. 1: The global phase diagram of 2D Dirac fermion system on the plane spanned by Coulomb interaction parameter α and on-site interaction parameter U . The critical line of U_c is taken from Ref. [17]. The solid part of the EI critical line is plotted based on our DS equation results, and the dashed part of this line is plotted based on extrapolation.

The results of Ref. [17], and also those of Ref. [18], are restricted to the region of weak Coulomb interaction. The region of strong Coulomb interaction appears to be inaccessible to the numerical methods developed in Ref. [17, 18]. As aforementioned, strong Coulomb interaction is able to induce excitonic gap generation. This problem has attracted broad interest in the past two decades. Extensive theoretical efforts have been devoted to examining whether the SM-EI transition takes place in graphene. In Refs. [17, 18], the influence of on-site interaction on SM-EI transition has not been addressed. Moreover, it remains unclear how the SM-EI transition is affected by the SM-AFM quantum criticality.

In this paper, we study the excitonic pairing of 2D Dirac fermions by considering both the Coulomb and on-site interactions. In particular, we investigate the impact of on-site interaction on the fate of excitonic pairing. For small values of U , the Coulomb interaction and on-site interaction need to be treated on equal footing. When U grows, the AFM correlation is gradually enhanced. As $U \rightarrow U_c$, the system approaches to the AFM QCP and the quantum fluctuation of AFM order parameter is coupled strongly to Dirac fermions. To examine the influence of AFM quantum criticality on excitonic pairing, we need to treat the interplay between the Coulomb interaction and the Yukawa coupling.

The non-perturbative Dyson-Schwinger (DS) equation approach will be employed to compute the excitonic gap and to determine α_c . In our calculations, the series expansion is controlled by the factor $1/N$, where N is the spin degeneracy of Dirac fermion. Thus the Coulomb interaction parameter α can take any value. This will allow us to access the strong Coulomb interaction regime. The Yukawa coupling between the AFM fluctuation and the Dirac fermion is also handled by the $1/N$ expansion. However, the on-site interaction is spin distinguished, to

be explained below, and $1/N$ expansion becomes invalid in this case. We will only consider weak on-site interaction and perform weak coupling expansion.

After taking into account the impact of weak on-site interaction, the critical value α_c for EI transition is only slightly increased. At the AFM QCP (U_c), α_c increases dramatically as the Yukawa coupling constant λ grows. Apparently, the excitonic gap generation is significantly suppressed by the quantum fluctuation of AFM order parameter. As U decreases from U_c , the system departs from the QCP and the suppression of excitonic pairing caused by the AFM fluctuation is gradually weakened. Combining these results with those reported in Ref. [17], we obtain a schematic global phase diagram on the U - α plane, shown in Fig. 1. It seems that the EI phase cannot be directly converted into the AFM Mott phase: they are separated by an intermediate SM phase.

A direct application of our results is that it offers a possible explanation of the discrepancy between recent theoretical finding and existing experiments in graphene. It is known that α takes its maximal value $\alpha = 2.16$ when graphene is suspended in vacuum. The zero-temperature ground state of suspended graphene should be an insulator if $\alpha_c < 2.16$. The values of α_c obtained by employing different approximations of DS equation are quite different. In a recent work, Carrington *et al.* [32] has gone beyond many of the previously used approximations, and found that $\alpha_c \approx 2.0$, slightly below $\alpha = 2.16$. This result suggests that suspended graphene may be an insulator at zero temperature. However, this is apparently at odds with experiments [20]. According to the analysis of Refs. [46], graphene seems to be close to the AFM QCP, thus the impact of AFM quantum criticality on α_c needs to be seriously taken into account. Our results show that the proximity to the AFM QCP significantly increases the critical value α_c , which makes SM-EI transition very unlikely to happen in realistic graphene.

The rest of the paper is organized as follows. In Sec. II, we present the DS equation for dynamical excitonic gap. The gap equation is solved and analyzed in Sec. III, and the physical application of the result is discussed in Sec. IV. The results are summarized in Sec. V.

II. DYSON-SCHWINGER GAP EQUATION

Free 2D Dirac fermion system is described by the Lagrangian in Minkowski space

$$\mathcal{L}_0 = \sum_{\sigma} \bar{\Psi}_{\sigma}(\tau, \mathbf{x}) (\gamma_0 \partial_0 - v \gamma_i \partial_i) \Psi_{\sigma}(\tau, \mathbf{x}), \quad (1)$$

where Ψ_{σ} is a four-component spinor field and $\bar{\Psi}_{\sigma} = \Psi_{\sigma}^{\dagger} \gamma_0$. The index σ sums from 1 to N , with $N = 2$ being the spin degeneracy of Dirac fermion. The 4×4 gamma matrices are defined via the standard Pauli matrices as $\gamma_{0,i} = \tau^3 \otimes (\sigma^3, i\sigma^2, -i\sigma^1)$, which satisfy the Clifford algebra. The fermion velocity v is taken to be a constant.

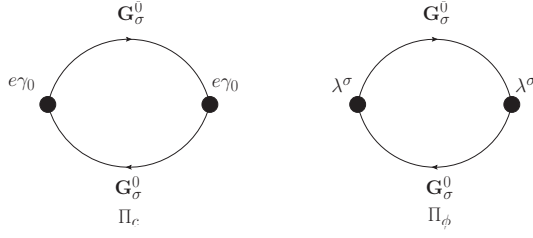


FIG. 2: Feynman diagram of Π_c and Π_ϕ . The difference between two diagrams lies in the expression of the vertices.

We will consider three different sorts of interactions, including the long-range Coulomb interaction, the spinful on-site interaction, as well as the Yukawa coupling between Dirac fermions and AFM quantum fluctuation. If the system is far from the AFM QCP, we only need to study the first two interactions. But when the system is sufficiently close to the AFM QCP, the interplay of Coulomb interaction and Yukawa coupling should be carefully investigated. Below we present the effective field theories for these three interactions in order.

A. Pure Coulomb interaction

The pure Coulomb interaction can be modeled by the following Lagrangian

$$\mathcal{L}_C = -ea_0 \sum_{\sigma} \bar{\Psi}_{\sigma} \gamma_0 \Psi_{\sigma} + a_0 \frac{|\nabla|^2}{2e^2} a_0, \quad (2)$$

where a_0 is an auxiliary scalar field introduced to represent Coulomb interaction. It is easy to verify that the Lagrangian $\mathcal{L}_0 + \mathcal{L}_C$ respects the continuous chiral symmetry $\Psi_{\sigma} \rightarrow e^{i\gamma_5 \theta} \Psi_{\sigma}$.

The pure Coulomb interaction has already been widely studied [21–26, 28, 31–34] previously. Here we only briefly summarize the main results for latter usage. As mentioned in Sec. I, the Coulomb interaction will be studied by employing the $1/N$ expansion. In this paper, we will retain the leading order contribution of $1/N$ expansion, and ignore the contribution of wave function renormalizations. The validity of this approximation will be discussed later. The free propagator of Dirac fermions is

$$G_{\sigma}^0(\omega, \mathbf{k}) = \frac{1}{\omega \gamma_0 - v(\gamma_1 k_x + \gamma_2 k_y)}. \quad (3)$$

Interaction corrections alters this propagator into

$$G_{\sigma}(\omega, \mathbf{k}) = \frac{1}{\omega \gamma_0 - v(\gamma_1 k_x + \gamma_2 k_y) - m_{\sigma}(\omega, \mathbf{k})}, \quad (4)$$

where $m_{\sigma}(\omega, \mathbf{k})$ is fermion self-energy function. Once $m_{\sigma}(\omega, \mathbf{k})$ acquires a finite value due to the Coulomb interaction, an excitonic mass gap is generated and the gapless SM is converted into a fully gapped EI. In order

to examine whether an excitonic gap is generated, we write down the following DS equation

$$m_{\sigma}(\varepsilon, \mathbf{p}) = \frac{1}{4} \int \frac{d\omega}{2\pi} \frac{d^2 \mathbf{k}}{(2\pi)^2} \text{Tr}[\gamma_0 G_{\sigma}(\omega, \mathbf{k}) \gamma_0 V(\Omega, \mathbf{q})], \quad (5)$$

where $\Omega = \varepsilon - \omega$ and $\mathbf{q} = \mathbf{p} - \mathbf{k}$. Here, the effective Coulomb interaction is given by

$$V(\Omega, \mathbf{q}) = \frac{1}{V_0^{-1}(\Omega, \mathbf{q}) - \Pi_c(\Omega, \mathbf{q})}, \quad (6)$$

where $\Pi_c(\Omega, \mathbf{q})$ is the polarization function and

$$V_0(\mathbf{q}) = \frac{2\pi e^2 \delta(t)}{\kappa |\mathbf{q}|} \quad (7)$$

is the bare Coulomb interaction, with $\kappa = \epsilon_0 \epsilon_r$ being the dielectric constant. To the leading order of $1/N$ expansion, the Feynman diagram for $\Pi_c(\Omega, \mathbf{q})$ is shown in Fig.2. At the random phase approximation (RPA) level, the one-loop Π_c is calculated as follows [21]

$$\begin{aligned} i\Pi_c(\Omega, \mathbf{q}) &= -N \int \frac{d\omega}{2\pi} \frac{d^2 \mathbf{k}}{(2\pi)^2} \text{Tr}[\gamma_0 G_0(\omega, \mathbf{k}) \gamma_0 \\ &\quad G_0(\omega + \Omega, \mathbf{k} + \mathbf{q})] \\ &= \frac{N}{8} \frac{\mathbf{q}^2}{\sqrt{v\mathbf{q}^2 - \Omega^2}}. \end{aligned} \quad (8)$$

After performing the Wick rotation ($\omega \rightarrow i\omega$), we get the following DS gap equation in Euclidean space [21]

$$\begin{aligned} m_{\sigma}(\varepsilon, \mathbf{p}) &= \int \frac{d\omega}{2\pi} \frac{d^2 \mathbf{k}}{(2\pi)^2} \frac{m_{\sigma}(\omega, \mathbf{k})}{\omega^2 + v^2 \mathbf{k}^2 + m_{\sigma}(\omega, \mathbf{k})^2} \\ &\quad \times \frac{1}{\frac{|\mathbf{q}|}{2\pi v\alpha} + \frac{N}{8} \frac{\mathbf{q}^2}{\sqrt{\Omega^2 + v^2 \mathbf{q}^2}}}. \end{aligned} \quad (9)$$

where a new parameter $\alpha = e^2/v\kappa$ is defined to measure the effective interaction strength. For a given flavor N , the above gap equation has a nontrivial solution, i.e., $m \neq 0$, only when $\alpha > \alpha_c$. The QCP between SM and EI phases is located at $\alpha = \alpha_c$. If the value of α is fixed, a nonzero gap could be generated only when $N < N_c$.

B. Weak on-site interaction

As showed by Herbut and his collaborators [11, 50], the generic on-site interaction is complex and can be decomposed into eight independent four-fermion coupling terms. Here, following Ref. [17], we only consider the spin-distinguished interaction term

$$\mathcal{L}_I = g \sum_{\sigma} (\sigma \bar{\Psi}_{\sigma} \Psi_{\sigma})^2, \quad (10)$$

which is responsible for the emergence of AFM Mott insulating phase. In Ref. [17], this is referred to as spinful

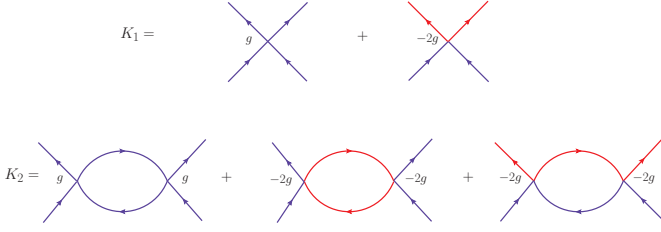


FIG. 3: Diagrams of leading (K_1) and sub-leading (K_2) order contributions to the GN interaction kernel. Blue solid line stands for fermions with spin σ , and red solid line for spin σ' .

Gross-Neveu (GN) interaction. It is also called chiral Heisenberg GN interaction [47]. According to Ref. [11], g is related to U through the identity $g = -\frac{Ua^2}{8}$.

Upon expanding the quadratic term appearing in \mathcal{L}_I , we get two sorts of four-fermion couplings

$$\mathcal{L}_I = g \sum_{\sigma} \bar{\Psi}_{\sigma} \Psi_{\sigma} \bar{\Psi}_{\sigma} \Psi_{\sigma} - 2g \bar{\Psi}_{\sigma_1} \Psi_{\sigma_1} \bar{\Psi}_{\sigma_2} \Psi_{\sigma_2}. \quad (11)$$

For a given spin σ , the coupling $\bar{\Psi}_{\sigma} \Psi_{\sigma} \bar{\Psi}_{\sigma} \Psi_{\sigma}$ amounts to the GN interaction with flavor $N = 1$. Such a coupling term cannot be treated by means of $1/N$ expansion. The coupling constant g has the dimension of inverse mass. It is convenient to define a dimensionless parameter $\tilde{g} = g\Lambda/v$, where the momentum cutoff Λ is connected to the lattice spacing a via the relation $\Lambda \sim a^{-1}$. In the following, we will choose to carry out series expansion in powers of \tilde{g} . This method is invalid in the strong coupling regime. Tang *et al.* [17] have numerically investigated the strong coupling regime by means of quantum MC simulation and found that the system enters into AFM Mott insulating phase once $|\tilde{g}|$ becomes sufficiently large.

We first ignore the Coulomb interaction and examine whether or not the pure GN interaction leads to dynamical generation of excitonic gap. According to the analysis of Ref. [48], the DS equation can be formally written as

$$G_{\sigma}^{-1} = (G_{\sigma}^0)^{-1} - \sum_{\sigma'} \text{Tr} [K_{\sigma,\sigma'} G_{\sigma'}] + \frac{1}{2} \sum_{\sigma'} \text{Tr} \left[G_{\sigma'} \frac{\delta K_{\sigma,\sigma'}}{\delta G_{\sigma}} G_{\sigma'} \right], \quad (12)$$

where $K_{\sigma,\sigma'}$ is the four-fermion interaction kernel. $K_{\sigma,\sigma'}$ can be obtained from the sum of all the two-particle irreducible vacuum diagrams in the full fermion propagators [48], represented by $V_{2\text{IR}}(G)$. $V_{2\text{IR}}(G)$ is connected to the kernel $K_{\sigma,\sigma'}$ in the following way

$$V_{2\text{IR}}(G) = \sum_{\sigma,\sigma'} \frac{1}{2} \text{Tr} [G_{\sigma} K_{\sigma,\sigma'} G_{\sigma'}]. \quad (13)$$

In this paper, we will retain both the leading order and sub-leading order corrections. The corresponding Feynman diagrams are presented in Fig. 3.

The leading order contributions to K are

$$(K_1)_{\sigma_1,\sigma_1} = \frac{v\tilde{g}}{\Lambda}, \quad (K_1)_{\sigma_1,\sigma_2} = -2\frac{v\tilde{g}}{\Lambda}. \quad (14)$$

The sub-leading order contributions are

$$\begin{aligned} (K_2)_{\sigma_1,\sigma_1}(q) &= - \int \frac{d^3k}{(2\pi)^3} \text{Tr} \left[\left(\frac{v\tilde{g}}{\Lambda} \right)^2 G_{\sigma_1}^0(k) G_{\sigma_1}^0(q+k) \right] \\ &\quad - \int \frac{d^3k}{(2\pi)^3} \text{Tr} \left[\left(2\frac{v\tilde{g}}{\Lambda} \right)^2 G_{\sigma_2}^0(k) G_{\sigma_2}^0(q+k) \right] \\ &= -5 \left(\frac{v\tilde{g}}{\Lambda} \right)^2 \Pi_g(q), \end{aligned} \quad (15)$$

$$\begin{aligned} (K_2)_{\sigma_1,\sigma_2}(q) &= - \int \frac{d^3k}{(2\pi)^3} \text{Tr} \left[\left(2\frac{v\tilde{g}}{\Lambda} \right)^2 G_{\sigma_1}^0(k) G_{\sigma_2}^0(q+k) \right] \\ &= -4 \left(\frac{v\tilde{g}}{\Lambda} \right)^2 \Pi_g(q), \end{aligned} \quad (16)$$

where $q \equiv (\Omega, \mathbf{q})$ and $k \equiv (\omega, \mathbf{k})$, and we define

$$\Pi_g(q) = \int \frac{d\omega}{2\pi} \frac{d^2\mathbf{k}}{(2\pi)^2} (2\pi)^3 \text{Tr} [G_{\sigma_i}^0(k) G_{\sigma_i}^0(q+k)], \quad (17)$$

which is independent of spin directions. After doing simple calculations, we find that $\Pi_g(q) = \frac{1}{4v^2} \sqrt{v^2 \mathbf{q}^2 - \Omega^2}$. From Fig. 3, we see that the first two orders of corrections satisfy the relation [48] $\frac{\delta K_i}{\delta G} = 0$ for both $i = 1$ and $i = 2$. Therefore, the DS equation for fermion self-energy takes the form

$$\begin{aligned} i\Sigma_{\sigma}(\varepsilon, \mathbf{p}) &= - \sum_{\sigma'} \int \frac{d\omega}{2\pi} \frac{d^2\mathbf{k}}{(2\pi)^2} \text{Tr} [i(K_1)_{\sigma,\sigma'}(\Omega, \mathbf{q}) iG_{\sigma'}(\omega, \mathbf{k})] + \sum_{\sigma'} \int \frac{d\omega}{2\pi} \frac{d^2\mathbf{k}}{(2\pi)^2} (i(K_2)_{\sigma,\sigma'}(\Omega, \mathbf{q})) (iG_{\sigma'}(\omega, \mathbf{k})) \\ &= -\frac{v\tilde{g}}{\Lambda} \int \frac{d\omega}{2\pi} \frac{d^2\mathbf{k}}{(2\pi)^2} \text{Tr} [G_{\sigma}(\omega, \mathbf{k})] + 9 \left(\frac{v\tilde{g}}{\Lambda} \right)^2 \int \frac{d\omega}{2\pi} \frac{d^2\mathbf{k}}{(2\pi)^2} (2\pi)^3 \Pi_g(\Omega, \mathbf{q}) G_{\sigma}(\omega, \mathbf{k}). \end{aligned} \quad (18)$$

In the small \tilde{g} region, we ignore the fermion damping and velocity renormalization, thus the fermion self-energy can be identified as the excitonic mass gap. Upon making Wick rotation, we derive the following DS gap equation

$$m_{\sigma}(\varepsilon, \mathbf{p}) = \frac{4v\tilde{g}}{\Lambda} \int \frac{d\omega}{2\pi} \frac{d^2\mathbf{k}}{(2\pi)^2} \frac{m_{\sigma}(\omega, \mathbf{k})}{\omega^2 + v^2 \mathbf{k}^2 + m_{\sigma}^2(\omega, \mathbf{k})} - \frac{9}{4v^2} \left(\frac{v\tilde{g}}{\Lambda} \right)^2 \int \frac{d\omega}{2\pi} \frac{d^2\mathbf{k}}{(2\pi)^2} \frac{m_{\sigma}(\omega, \mathbf{k}) \sqrt{v^2 \mathbf{q}^2 + \Omega^2}}{\omega^2 + v^2 \mathbf{k}^2 + m_{\sigma}^2(\omega, \mathbf{k})}. \quad (19)$$

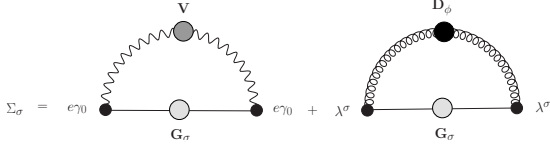


FIG. 4: Feynman diagram of fermion self-energy.

The leading order correction to dynamical gap generation has been previously analyzed in Ref. [49]. Notice there is a sign difference in the definition of \tilde{g} . In Ref. [49], a finite gap is generated only when $\tilde{g} < \tilde{g}_c = -\pi^2/4$ (in the limit of $N \rightarrow \infty$); in our case the critical value becomes $\tilde{g}_c = \pi^2/2$. In this work we only consider negative \tilde{g} , thus the GN interaction cannot induce excitonic pairing by itself. However, the GN interaction might affect the fate of excitonic pairing induced by the Coulomb interaction. This will be studied in Sec. III A.

C. Yukawa coupling near AFM QCP

When the strength of spinful GN interaction increases, the AFM correlation is enhanced. The gapless Dirac SM would become an AFM Mott insulator once U exceeds some critical value U_c , which defines a zero temperature AFM QCP. As revealed by Tang *et al.* [17], U_c appears to be an increasing function of α in the region of weak Coulomb interaction. Previous studies on such an AFM quantum criticality [11, 50] revealed that the Yukawa coupling between Dirac fermions and the AFM quantum critical fluctuation, described by scalar field ϕ , determines the low-energy properties of the AFM quantum critical phenomena if Coulomb interaction is ignored. Here, we are particularly interested in whether the excitonic pairing is suppressed or promoted near the AFM QCP.

To describe the AFM fluctuation, we add to \mathcal{L}_0 the following additional terms

$$\mathcal{L}_b = -\phi(\partial_\tau^2 + v_\phi^2 \nabla^2 + r)\phi - \frac{\lambda_0}{4!}\phi^4 + \sum_\sigma \lambda\phi \cdot \sigma \bar{\Psi}_\sigma \Psi_\sigma \quad (20)$$

where λ is the strength parameter for Yukawa coupling and $\sigma = \pm 1$ is fermion spin. The AFM order parameter [11, 17] is given by $A = \langle \sum_\sigma \sigma \bar{\Psi}_\sigma \Psi_\sigma \rangle$. The scalar field ϕ stands for the quantum fluctuation around this mean value. The boson mass r can be identified as the tuning parameter for SM-AFM transition, and $r = 0$ at the QCP

g_c . Here, we only consider the SM side of the QCP, and thus suppose $r \geq 0$. To facilitate analytical calculations, we introduce two new coupling constants for two spin components: $\lambda_\sigma = \lambda\sigma$. It is worth mentioning that λ_σ have the same dimension as \sqrt{r} .

Once \mathcal{L}_b is introduced, the continual chiral symmetry is explicitly broken. Nevertheless, the total action still preserves a discrete chiral symmetry $\Psi_\sigma \rightarrow \gamma_5 \Psi_\sigma$, so long as the scalar field ϕ transforms simultaneously in the following way: $\phi \rightarrow -\phi$. If a finite gap is generated, the above discrete chiral symmetry will be broken.

The Feynman diagrams of the fermion self-energy are shown in Fig. 4, where V stands for the dressed Coulomb interaction function and D_ϕ for the dressed propagator of the ϕ field. To the leading order of $1/N$ expansion, we need to consider the following DS equation

$$m_\sigma(\varepsilon, \mathbf{p}) = \frac{i}{4} \int \frac{d\omega}{2\pi} \frac{d^2\mathbf{k}}{(2\pi)^2} \text{Tr}[\gamma_0 G_\sigma(\omega, \mathbf{k}) V(\Omega, \mathbf{q}) \gamma_0] + \frac{i(\lambda_\sigma)^2}{4} \int \frac{d\omega}{2\pi} \frac{d^2\mathbf{k}}{(2\pi)^2} \text{Tr}[G_\sigma(\omega, \mathbf{k}) D_\phi(\Omega, \mathbf{q})], \quad (21)$$

where $\varepsilon = \Omega + \omega$ and $\mathbf{p} = \mathbf{q} + \mathbf{k}$.

The free propagator of ϕ is $D_\phi^0(\Omega, \mathbf{q}) = \frac{1}{\Omega^2 - \mathbf{q}^2 - r^2}$. Similar to the Coulomb interaction, this free propagator is also renormalized by collective excitations. Including this effect leads to a dressed bosonic propagator

$$D_\phi(\Omega, \mathbf{q}) = \frac{1}{D_\phi^0(\Omega, \mathbf{q})^{-1} + \Pi_\phi(\Omega, \mathbf{q})}, \quad (22)$$

in which the polarization function Π_ϕ , whose diagram is presented in Fig. 2, is given by

$$\Pi_\phi(\Omega, \mathbf{q}) = - \sum_\sigma \int \frac{d\omega}{2\pi} \frac{d^2\mathbf{k}}{(2\pi)^2} \text{Tr}[\lambda_\sigma G_\sigma^0(\omega, \mathbf{k}) \lambda_\sigma \times G_\sigma^0(\omega + \Omega, \mathbf{k} + \mathbf{q})] \quad (23)$$

to the leading order of $1/N$ expansion. According to the detailed derivation shown in Appendix. A, we find

$$\Pi_\phi(\Omega, \mathbf{q}) = - \frac{N(\lambda_\sigma)^2}{v^2} \frac{\sqrt{v^2 \mathbf{q}^2 - \Omega^2}}{4}. \quad (24)$$

After performing a series of analytical calculations, we arrive at the following gap equation

$$m_\sigma(\varepsilon, \mathbf{p}) = \int \frac{d\omega}{2\pi} \frac{d^2\mathbf{k}}{(2\pi)^2} \frac{m_\sigma(\omega, \mathbf{k})}{\omega^2 + v^2 \mathbf{k}^2 + m_\sigma(\omega, \mathbf{k})^2} \frac{1}{\frac{|\mathbf{q}|}{2\pi v \alpha} + \frac{N}{8} \frac{\mathbf{q}^2}{\sqrt{\Omega^2 + v^2 \mathbf{k}^2}}} - (\lambda_\sigma)^2 \int \frac{d\omega}{2\pi} \frac{d^2\mathbf{k}}{(2\pi)^2} \frac{m_\sigma(\omega, \mathbf{k})}{\omega^2 + v^2 \mathbf{k}^2 + m_\sigma(\omega, \mathbf{k})^2} \frac{1}{\Omega^2 + \mathbf{q}^2 + r^2 + \frac{N(\lambda_\sigma)^2}{v^2} \frac{\sqrt{\Omega^2 + v^2 \mathbf{q}^2}}{4}}, \quad (25)$$

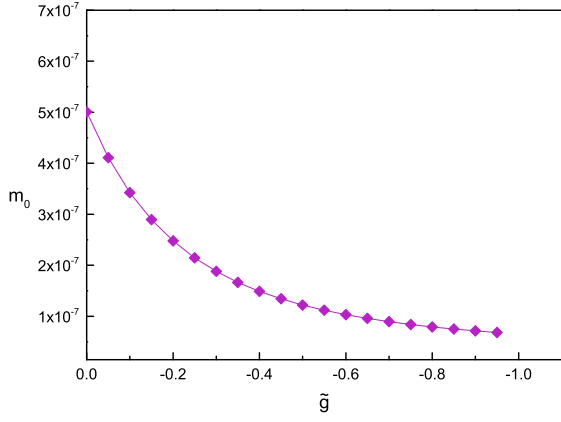


FIG. 5: The \tilde{g} -dependence of zero-momentum excitonic gap m_0 at $\alpha = 2.2$ and $N = 2$.

where the Wick rotation has been performed. There is a minus sign in the contribution due to the Yukawa coupling. Two important facts can be deduced. First, the Yukawa coupling tends to suppress excitonic pairing. Second, the Yukawa coupling by itself is not able to trigger excitonic pairing.

III. NUMERICAL RESULTS

In this section, we solve the DS equations numerically and analyze the physical implications of the solutions. We will first consider the case of weak GN interaction and then the vicinity of AFM QCP. Our aim is to determine their influence on the value of α_c .

A. Interplay of Coulomb and GN interactions

To examine the interplay between the long-range Coulomb and short-range GN interactions, we combine Eq. 9 and Eq. 19, and then solve the total gap equation self-consistently for different values of \tilde{g} at $N = 2$ and $\alpha = 2.2$ (the physical value of α in suspended graphene). The energy cutoff is chosen as $\Lambda_E = v\Lambda$.

To simplify numerical evaluation, it is useful to first adopt the commonly used instantaneous approximation [21], which assumes that the fermion gap and Coulomb interaction are independent of energy. The impact of energy dependence will be examined later. Under this approximation, the total gap equation has the form

$$m_\sigma(\mathbf{p}) = \int \frac{d^2\mathbf{k}}{(2\pi)^2} \frac{m_\sigma(\mathbf{k})}{2\sqrt{v^2\mathbf{k}^2 + m_\sigma^2(\mathbf{k})^2}} \frac{1}{\frac{|\mathbf{q}|}{2\pi v\alpha} + \frac{N}{8} \frac{|\mathbf{q}|}{v}} + \frac{v\tilde{g}}{\Lambda} \int \frac{d^2\mathbf{k}}{(2\pi)^2} \frac{m_\sigma(\mathbf{k})}{2\sqrt{v^2\mathbf{k}^2 + m_\sigma^2(\mathbf{k})^2}} - \frac{9}{4v} \left(\frac{v\tilde{g}}{\Lambda} \right)^2 \int \frac{d^2\mathbf{k}}{(2\pi)^2} \frac{|\mathbf{q}| m_\sigma(\mathbf{k})}{2\sqrt{v^2\mathbf{k}^2 + m_\sigma^2(\mathbf{k})^2}} \quad (26)$$

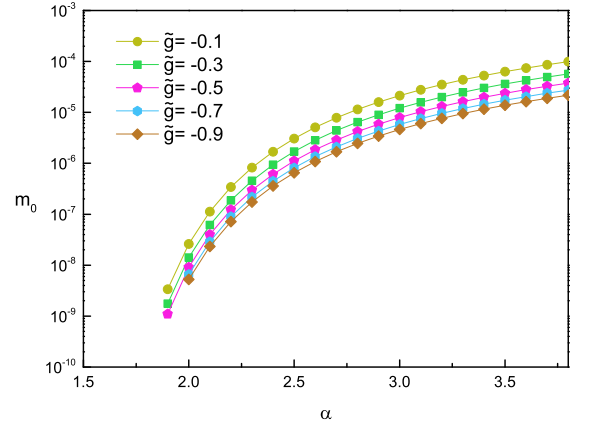


FIG. 6: The α -dependence of zero-momentum gap m_0 for different values of $v\tilde{g}$ at $N = 2$.

After solving this equation, we present the numerical results in Fig. 5, where m_0 is defined as the value of fermion gap at zero energy and zero momentum. As $|\tilde{g}|$ grows, m_0 decreases considerably. This implies that weak GN interaction tends to suppress excitonic gap. The α -dependence of m_0 is shown in Fig. 6. We observe that, as GN interaction is becoming stronger, the value of α_c is slightly increased. In particular, for $\tilde{g} = -0.7$, $\alpha_c = 2.0$.

The instantaneous approximation has been previously used in the DS study of excitonic gap generation [21]. More refined works [32] have confirmed that the value of α_c obtained under this approximation is actually not far from the one obtained by incorporating higher order corrections. In this regard, the instantaneous approximation leads to qualitatively reliable conclusion. We have solved the gap equation after incorporating the energy dependence of gap function and Coulomb interaction, and found that the qualitative conclusions are the same but the concrete values of \tilde{g}_c and α_c are more or less changed.

B. Interplay of Coulomb interaction and Yukawa coupling

We now consider the interplay of Coulomb interaction and Yukawa coupling. The corresponding DS gap equation is given by Eq. 25. To obtain the numerical results, a renormalization procedure has to be taken, in which the dimension of all parameters will be eliminated by dividing either Λ or Λ_E . The parameters appears blow are renormalized without explicitly statement. To get a rapid glimpse of the main results, we first neglect the energy dependence of fermion self-energy and interaction functions, which leads to

$$m_\sigma(\varepsilon, \mathbf{p}) \rightarrow m_\sigma(\mathbf{p}), \quad (27)$$

$$V(\Omega, \mathbf{q}) \rightarrow V(\mathbf{q}), \quad (28)$$

$$D_\phi(\Omega, \mathbf{q}) \rightarrow D_\phi(\mathbf{q}). \quad (29)$$

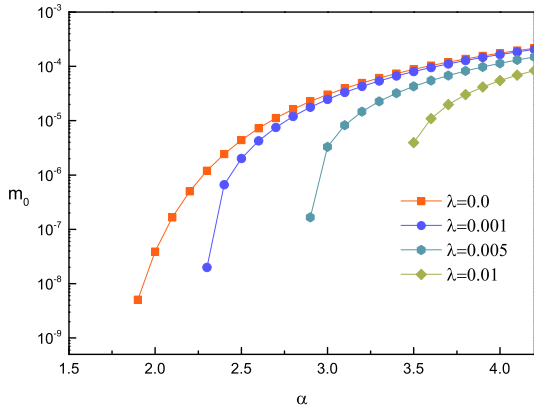


FIG. 7: The α -dependence of m_0 for different values of λ at $N = 2$. Clearly, α_c is an increasing function of λ .

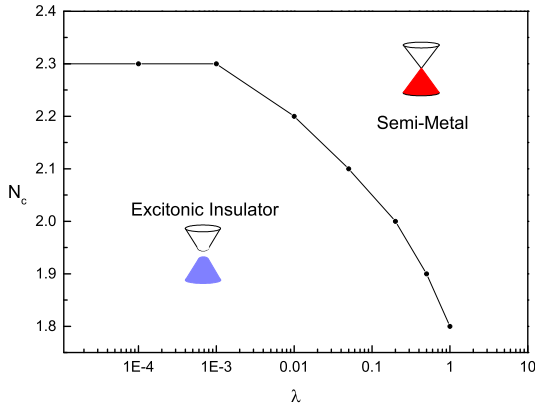


FIG. 8: The critical line of SM-EI transition on the λ - N plane. Here the Coulomb interaction parameter is fixed at $\alpha = 3.2$.

Now DS gap equation is simplified to

$$m_\sigma(\mathbf{p}) = \int \frac{d^2\mathbf{k}}{(2\pi)^2} \frac{m_\sigma(\mathbf{k})}{2\sqrt{v^2\mathbf{k}^2 + m_\sigma(\mathbf{k})^2}} \frac{1}{\frac{|\mathbf{q}|}{2\pi v\alpha} + \frac{N}{8} \frac{|\mathbf{q}|}{v}} - (\lambda_\sigma)^2 \int \frac{d^2\mathbf{k}}{(2\pi)^2} \frac{m_\sigma(\mathbf{k})}{2\sqrt{v^2\mathbf{k}^2 + m_\sigma(\mathbf{k})^2}} \times \frac{1}{\mathbf{q}^2 + r^2 + \frac{N(\lambda_\sigma)^2}{v} \frac{|\mathbf{q}|}{4}}. \quad (30)$$

We have solved this equation numerically, and now show in Fig. 7 the α -dependence of excitonic gap obtained at zero momenta, namely $m(p=0)$, for different values of λ . If the AFM QCP is entirely ignored, corresponding to $\lambda = 0$, the critical value $\alpha_c \approx 1.9$. If λ takes a very small value $\lambda = 0.001$, α_c is increased to $\alpha_c \approx 2.3$. For $\lambda = 0.005$ and $\lambda = 0.01$, we find that $\alpha_c = 2.8$ and $\alpha_c = 3.5$, respectively. Therefore, the excitonic gap generation can be significantly suppressed at the AFM QCP.

Further, we study how λ changes the critical fermion flavor N_c . We fix α at $\alpha = 3.2$, and solve Eq. (34) to obtain the relation between λ and N_c , with results presented in Fig. 8. For very small values of λ , $N_c \approx 2.3$. For

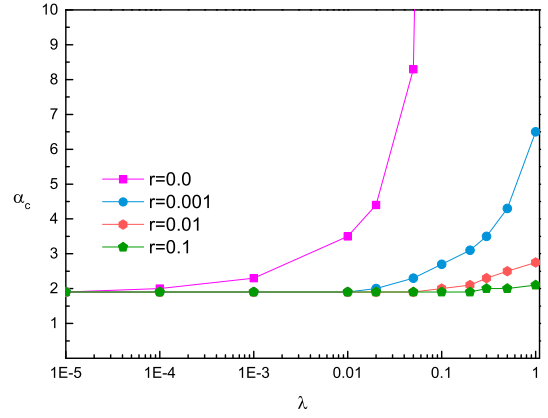


FIG. 9: The λ -dependence of α_c at a number of values of r . Here the fermion flavor is $N = 2$.

$\lambda > 0.2$, N_c is reduced below 2. For a Dirac fermion with physical flavor $N = 2$, excitonic pairing is completely forbidden in the presence of sufficiently strong Yukawa coupling.

The dependence of α_c on λ at fixed flavor $N = 2$ is shown in Fig. 9. At the AFM QCP with $r = 0$, α_c increases rapidly as λ grows, and finally goes to infinity at sufficiently large λ . This is another signature that AFM quantum criticality disfavors excitonic gap generation. As r increases, the system moves away from the AFM QCP into the SM region. In this process, the quantum fluctuation of AFM order parameter is weakened, and the suppressing effect of excitonic pairing becomes progressively unimportant.

In Ref. [17], the authors revealed that Coulomb interaction tends to increase U_c . Here we have showed that AFM quantum fluctuation can suppress excitonic pairing. There seems to be a repulsion between the excitonic pairing and the AFM ordering. Based on these results, we plot a schematic phase diagram on the U - α plane in Fig. 1. The critical line of U_c goes rightwards as α increases [17], whereas the critical line of α_c goes upwards as $U \rightarrow U_c$ from the left side. A previous RG study [11] predicted that the Dirac fermion system may undergo a first-order transition from EI to AFM Mott insulator. Our results indicate that such a direct transition does occur, and that the excitonic insulating phase and AFM Mott insulating phase are actually separated by an intermediate gapless SM phase.

We have also numerically solved Eq. (30) after including the retardation effects ($\alpha_c = 0.7$ at $\lambda = 0$) and reached the same conclusion that the quantum AFM criticality suppresses excitonic gap generation. Therefore, the schematic phase diagram presented in Fig. 1 is still qualitatively correct after taking the energy dependence into account.

IV. APPLICATION OF THE RESULTS

Determination of the precise value of α_c proves to be a highly nontrivial challenge. In QED₃ and QED₄, the fermion propagator, the gauge boson propagator, and the fermion-boson vertex function form a closed set of integral equations [51]. This result is valid in our case because the Coulomb interaction can be effectively described by the interaction between the Dirac fermion and the temporal component of U(1) gauge boson. The full fermion propagator has the generic form

$$G(\varepsilon, \mathbf{p}) = \frac{1}{\gamma_0 \varepsilon Z(\varepsilon, \mathbf{p}) - v(\gamma_1 p_x + \gamma_2 p_y) A(\varepsilon, \mathbf{p}) - m(\varepsilon, \mathbf{p})},$$

where $Z(\varepsilon, \mathbf{p})$ and $A(\varepsilon, \mathbf{p})$ are the wave function renormalizations and $m(\varepsilon, \mathbf{p})$ is the fermion gap function. The full boson propagator is given by Eq. 6, and the vertex function can be represented by Γ . The DS equations contain all the information caused by interactions. Once the complete expression for the vertex function is derived, the full fermion and boson propagators can be determined. In practice, it is not possible to obtain the exact solutions of DS equations, and one always needs to introduce certain approximations (truncations) to replace full propagators and/or full vertex function. There are two commonly used vertex functions: the bare vertex and the Ball-Chiu [52] vertex.

Extensive DS equation studies of excitonic pairing in graphene have showed that the value of α is very sensitive to the specific approximation. To demonstrate this, we list in Table I a number of representative values of α_c obtained by employing various approximations. If one assumes $Z = A = 1$ and ignores vertex correction, $\alpha_c = 1.9$ in the instantaneous approximation and $\alpha_c = 0.7$ after including the energy dependence. Two of the authors incorporated Z and A , utilized the first term of Ball-Chiu vertex, and adopted the RPA expression of polarization Π_c , and found [28] $\alpha \approx 3.2$. It was pointed out in Ref. [28] that α_c could be considerably decreased if the feedback of excitonic gap on Π_c is included. Recently, Carrington *et al.* [32] have carried out carefully DS equation calculations after taken into account Z and A , the first term of Ball-Chiu vertex, and also the feedback of Z , A , and m on Π_c , and obtained $\alpha_c \approx 2.06$. It is surprising that the value $\alpha_c = 1.9$ obtained in the present paper by using the very crude instantaneous approximation is actually quite close to the above result. Moreover, the α_c obtained by Carrington *et al.* [32] is smaller than the physical value $\alpha = 2.16$ of suspended graphene. In the light of this result, one might have to conclude that clean, undoped suspended graphene is an EI at low temperatures.

Ellias *et al.* [20] has measured the cyclotron mass in suspended graphene and found no evidence of finite gap at rather low energies ($\sim 0.1\text{meV}$). This finding was further supported by the measurements of Mayorov *et al.* [53]. How can one reconcile the recent theoretical result of Carrington *et al.* [32] and these experiments?

TABLE I: DS equation results for the critical value α_c at the flavor $N = 2$. Z , A , m , and α are defined in the context. Γ_{BC} stands for the Ball-Chiu vertex correction. Π_c^{RPA} is the RPA-level polarization given by Eq. (8), and Π_c^{SC} represents the polarization function obtained from self-consistent DS equation calculations. The symbol \otimes refers to the instantaneous approximation, and \checkmark indicates that the energy dependence is taken into account. The corresponding function is neglected if the space is left blank.

Z	A	m	Γ_{BC}	Π_c^{SC}	Π_c^{RPA}	α	Reference
		\otimes			\checkmark	1.9	current paper
		\otimes			\checkmark	0.92	[34]
		\otimes			\checkmark	0.7	current paper
\checkmark	\checkmark	\checkmark	\checkmark		\checkmark	3.2	[28]
\checkmark	\checkmark	\checkmark	\checkmark		\checkmark	2.9	[31]
\checkmark	\checkmark	\checkmark	\checkmark	\otimes		1.99	[32]
\checkmark	\checkmark	\checkmark	\checkmark	\checkmark		2.06	[32]

Here we propose that the seeming discrepancy can be explained by noting the fact that graphene is not far from the AFM QCP. Wehling *et al.* [46] has calculated the on-site interaction parameter U by using three different approaches. The critical value U_c needed to trigger AFM Mott transition seems to be only slightly larger than the physical U [17], which implies that realistic graphene is close to the AFM QCP [17]. Apparently, the AFM quantum fluctuation is important in graphene and should be seriously considered in the study of the EI transition. As revealed in our calculations, AFM quantum fluctuation can strongly suppress excitonic pairing by increasing the value of α_c . Therefore, we conclude that the gapless SM state of suspended graphene is actually quite robust.

V. SUMMARY AND DISCUSSION

In summary, we have investigated the non-perturbative effect of dynamical excitonic gap generation in a 2D Dirac fermion system. The Dirac fermions are subjected to two types of interaction, namely the long-range Coulomb interaction and the short-range on-site interaction. The former interaction can trigger excitonic pairing, whereas the latter leads to AFM quantum phase transition in the strong coupling regime. The DS equation approach is employed to study the influence of GN-type on-site interaction on the fate of SM-EI transition. We first have showed that the GN interaction only leads to weak suppression of excitonic gap generation. As the system approaches to the AFM QCP, the dynamics of Dirac fermions is strongly influenced by the quantum critical fluctuation of AFM order parameter. We have demonstrated that excitonic gap generation is suppressed by AFM quantum fluctuation. Such a suppression effect is most significant at the AFM QCP, but gradually diminishes when the system moves away from the QCP. If 2D Dirac fermion

system is close to the AFM QCP, as what happens in graphene, it would be very difficult to realize excitonic pairing.

Based on these results, we provide supplementary new information to the global phase diagram reported in Ref. [17]. On the phase diagram, the EI phase is not neighboring to the AFM phase, but is separated from the AFM phase by an intermediate SM phase, as illustrated schematically in Fig. 11. This conclusion is different from the one previously reported in Ref. [11]. Our results indicates that it is hardly possible to transform 2D Dirac fermion system from an EI phase directly to AFM Mott phase. The reason is that the quantum critical AFM fluctuation prevents excitonic pairing.

When both α and U take large values, the Dirac fermion system could either be a AFM Mott insulator

or enters into a CDW phase due to excitonic pairing, or remain as a semimetal. To determine the quantitatively more precise phase diagram in such a highly interacting regime, it is necessary to investigate the mutual influence between strong Coulomb interaction and strong on-site interaction in a more self-consistent manner, which will be carried out in future works.

Acknowledgments

The authors acknowledge the financial support by the National Natural Science Foundation of China under Grants 11847234, 11574285, and 11504379.

Appendix A: Calculation of the polarization Π_ϕ

We now provide the calculational details of the polarization function for the dressed propagator of bosonic AFM fluctuation. To the leading order of $1/N$ expansion, this polarization is defined as

$$\begin{aligned} i\Pi_\phi(\Omega, \mathbf{q}) &= - \sum_\sigma \int \frac{d\omega}{2\pi} \frac{d^2\mathbf{k}}{(2\pi)^2} \text{Tr}[\lambda_\sigma G_\sigma^0(\omega, \mathbf{k}) \lambda_\sigma G_\sigma^0(\omega + \Omega, \mathbf{k} + \mathbf{q})] \\ &= - \sum_\sigma \int \frac{d\omega}{2\pi} \frac{d^2\mathbf{k}}{(2\pi)^2} \text{Tr} \left[\lambda_\sigma \frac{1}{-\gamma_0\omega + v\gamma\mathbf{k} + m_e} \lambda_\sigma \frac{1}{-\gamma_0(\omega + \Omega) + v\gamma(\mathbf{k} + \mathbf{q}) + m_e} \right], \end{aligned} \quad (\text{A1})$$

where m_e is a constant mass of Dirac fermion. Making the replacements $\mathbf{q} = v\mathbf{q}$ and $\mathbf{k} = v\mathbf{k}$, we re-write it in the form

$$\begin{aligned} i\Pi_\phi(\Omega, \mathbf{q}) &= - \sum_\sigma \int \frac{d\omega}{2\pi} \frac{d^2\mathbf{k}}{(2\pi)^2} \text{Tr} \left[\frac{\lambda_\sigma}{v^2} \frac{1}{-\gamma_0\omega + \gamma\mathbf{k} + m_e} \lambda_\sigma \frac{1}{-\gamma_0(\omega + \Omega) + \gamma(\mathbf{k} + \mathbf{q}) + m_e} \right] \\ &= -4 \sum_\sigma \left(\frac{\lambda_\sigma}{v} \right)^2 \int \frac{d\omega}{2\pi} \frac{d^2\mathbf{k}}{(2\pi)^2} \frac{((\Omega + \omega)\omega - (\mathbf{k} + \mathbf{q}) \cdot \mathbf{k} + m_e^2)}{((\Omega + \omega)^2 - (\mathbf{k} + \mathbf{q})^2 - m_e^2)(\omega^2 - \mathbf{k}^2 - m_e^2)}. \end{aligned} \quad (\text{A2})$$

Making use of the Feynman integral

$$\frac{1}{AB} = \int_0^1 dx \frac{1}{[(1-x)A + xB]^2}, \quad (\text{A3})$$

we proceed as follows

$$\begin{aligned} i\Pi_\phi &= -4 \sum_\sigma \left(\frac{\lambda_\sigma}{v} \right)^2 \int_0^1 dx \int \frac{d\omega}{2\pi} \frac{d^2\mathbf{k}}{(2\pi)^2} \frac{((\Omega + \omega)\omega - (\mathbf{k} + \mathbf{q}) \cdot \mathbf{k} + m_e^2)}{(x(\Omega + \omega)^2 - x(\mathbf{k} + \mathbf{q})^2 - xm_e^2 + (1-x)\omega^2 - (1-x)\mathbf{k}^2 - (1-x)m_e^2)^2} \\ &= -4 \sum_\sigma \left(\frac{\lambda_\sigma}{v} \right)^2 \int_0^1 dx \int \frac{d\omega}{2\pi} \frac{d^2\mathbf{k}}{(2\pi)^2} \frac{((\Omega + \omega)\omega - (\mathbf{k} + \mathbf{q}) \cdot \mathbf{k} + m_e^2)^2}{((x-x^2)(\Omega^2 - \mathbf{q}^2) + (\omega + x\Omega)^2 - (\mathbf{k} + x\mathbf{q})^2 - m_e^2)^2}. \end{aligned} \quad (\text{A4})$$

Define $\omega' = \omega + x\Omega$ and $\mathbf{k}' = \mathbf{k} + x\mathbf{q}$, we further get

$$\begin{aligned} i\Pi_\phi &= -4 \sum_\sigma \left(\frac{\lambda_\sigma}{v} \right)^2 \int_0^1 dx \int \frac{d\omega'}{2\pi} \frac{d^2\mathbf{k}'}{(2\pi)^2} \frac{(\omega' - x\Omega)(\omega' + (1-x)\Omega) - (\mathbf{k}' + (1-x)\mathbf{q}) \cdot (\mathbf{k}' - x\mathbf{q}) + m_e^2}{((x-x^2)(\Omega^2 - \mathbf{q}^2) + (\omega')^2 - \mathbf{k}'^2 - m_e^2)^2} \\ &= -4 \sum_\sigma \left(\frac{\lambda_\sigma}{v} \right)^2 \int_0^1 dx \int \frac{d\omega'}{2\pi} \frac{d^2\mathbf{k}'}{(2\pi)^2} \frac{\omega'^2 + (1-2x)\Omega\omega' - x(1-x)\Omega^2 - \mathbf{k}'^2 - (1-2x)\mathbf{q} \cdot \mathbf{k}' + x(1-x)\mathbf{q}^2 + m_e^2}{((x-x^2)(\Omega^2 - \mathbf{q}^2) + \omega'^2 - \mathbf{k}'^2 - m_e^2)^2}. \end{aligned} \quad (\text{A5})$$

Introducing $C = \sqrt{(x - x^2)(\Omega^2 - \mathbf{q}^2) - \mathbf{k}'^2 - m_e^2}$ leads to

$$i\Pi_\phi = 4 \sum_\sigma \left(\frac{\lambda_\sigma}{v} \right)^2 \int_0^1 dx \int \frac{d\omega'}{2\pi} \frac{d^2\mathbf{k}'}{(2\pi)^2} \left[\frac{\omega'^2}{(\omega'^2 + C^2)^2} - \frac{(x - x^2)(\Omega^2 - \mathbf{q}^2) + \mathbf{k}'^2 - m_e^2}{(\omega'^2 + C^2)^2} \right].$$

Since

$$\int_{-\infty}^{+\infty} dx \frac{x^2}{(x^2 + a^2)^2} = \frac{\pi}{2a}, \quad \int_{-\infty}^{+\infty} dx \frac{1}{(x^2 + a^2)^2} = \frac{\pi}{2a^3}, \quad (\text{A6})$$

we find that

$$\begin{aligned} i\Pi_\phi &= -4 \sum_\sigma \left(\frac{\lambda_\sigma}{v} \right)^2 \int_0^1 dx \int \frac{d^2\mathbf{k}'}{(2\pi)^3} \left[\frac{\pi}{2C} - \frac{\pi[C^2 + 2\mathbf{k}'^2]}{2C^3} \right] \\ &= 4 \sum_\sigma \left(\frac{\lambda_\sigma}{v} \right)^2 \int_0^1 dx \int \frac{d^2\mathbf{k}'}{(2\pi)^3} \frac{2\pi\mathbf{k}'^2}{2\sqrt{((x - x^2)(\Omega^2 - \mathbf{q}^2) - \mathbf{k}'^2 - m_e^2)^3}}. \end{aligned}$$

After carrying out a series of calculations, we eventually obtain

$$i\Pi_\phi = -\frac{iN(\lambda_\sigma)^2}{8v^2} \left[\Lambda - 2\sqrt{\mathbf{q} - \Omega^2 - m_e^2} \right], \quad (\text{A7})$$

where Λ is an UV cutoff. In the massless limit, i.e., $m_e = 0$, we have

$$\Pi_\phi = -\frac{N(\lambda_\sigma)^2}{4v^2} \sqrt{v^2\mathbf{q} - \Omega^2}. \quad (\text{A8})$$

After Wick rotation ($\Omega \rightarrow i\Omega$), we can have the polarization function in Euclidean space

$$\Pi_\phi^E = -\frac{N(\lambda_\sigma)^2}{4v^2} \sqrt{v^2\mathbf{q} + \Omega^2}. \quad (\text{A9})$$

-
- [1] P. A. Lee, N. Nagaosa, and X.-G. Wen, *Rev. Mod. Phys.* **78**, 17 (2006).
 - [2] J. Orenstein and A. J. Millis, *Science* **288**, 468 (2000).
 - [3] K. S. Novoselov, A. K. Geim, S. V. Morozov, D. Jiang, Y. Zhang, S. V. Dubonos, I. V. Grigorieva, and A. A. Firsov, *Science* **306**, 666 (2004).
 - [4] K. S. Novoselov, A. K. Geim, S. V. Morozov, D. Jiang, M. I. Katsnelson, I. V. Grigorieva, S. V. Dubonos, and A. A. Firsov, *Nature (London)* **438**, 197 (2005).
 - [5] A. H. Castro Neto, F. Guinea, N. M. R. Peres, K. S. Novoselov, and A. K. Geim, *Rev. Mod. Phys.* **81**, 109 (2009).
 - [6] S. Das Sarma, S. Adam, E. H. Hwang, and E. Rossi, *Rev. Mod. Phys.* **83**, 407 (2011).
 - [7] V. N. Kotov, B. Uchoa, V. M. Pereira, A. H. Castro Neto, and F. Guinea, *Rev. Mod. Phys.* **83**, 407 (2011).
 - [8] M. Z. Hasan and C. L. Kane, *Rev. Mod. Phys.* **82**, 3045 (2010).
 - [9] M. Hirata, K. Ishikawa, K. Miyagawa, M. Tamura, C. Berthier, D. Basko, A. Kobayashi, G. Matsuno, and K. Kanoda, *Nature Commun.* **7**, 12666 (2016).
 - [10] R. Shankar, *Rev. Mod. Phys.* **66**, 129 (1994).
 - [11] I. F. Herbut, *Phys. Rev. Lett.* **97**, 146401 (2006).
 - [12] T. Sato, M. Hohenadler, and F. F. Assaad, *Phys. Rev. Lett.* **119**, 197203 (2017).
 - [13] S. Raghu, X.-L. Qi, C. Honerkamp, and S.-C. Zhang, *Phys. Rev. Lett.* **100**, 156401 (2008).
 - [14] C. Weeks and M. Franz, *Phys. Rev. B* **81**, 085105 (2010).
 - [15] A. G. Grushin, E. V. Castro, A. A. Cortijo, F. de Juan, M. A. H. Vozmediano, and B. Valenzuela, *Phys. Rev. B* **87**, 085136 (2013).
 - [16] M. Daghofer and M. Hohenadler, *Phys. Rev. B* **89**, 035103 (2014).
 - [17] H.-K. Tang, J. N. Leaw, J. N. B. Rodrigues, I. Herbut, P. Sengupta, F. F. Assaad, and S. Adam, *Science* **361**, 570 (2018).
 - [18] P. Buividovich, D. Smith, M. Ulybyshev, and L. von Smekal, *Phys. Rev. B* **98**, 235129 (2018).
 - [19] T.-S. Zeng, W. Zhu, and D. Sheng, *npj Quant Mater* **3**, 49 (2018).
 - [20] D. C. Elias, R. V. Gorbachev, A. S. Mayorov, S. V. Morozov, A. A. Zhukov, P. Blake, L. A. Ponomarenko, I. V. Grigorieva, K. S. Novoselov, F. Guinea, and A. K. Geim, *Nat. Phys.* **7**, 701 (2011).

- [21] D. V. Khveshchenko, Phys. Rev. Lett. **87**, 246802 (2001).
- [22] E. V. Gorbar, V. P. Gusynin, V. A. Miransky, and I. A. Shovkovy, Phys. Rev. B **66**, 045108 (2002).
- [23] D. V. Khveshchenko and H. Leal, Nucl. Phys. B **687**, 323 (2004).
- [24] G.-Z. Liu, W. Li, and G. Cheng, Phys. Rev. B **79**, 205429 (2009).
- [25] D. V. Khveshchenko, J. Phys.: Condens. Matter **21**, 075303 (2009).
- [26] O. V. Gamayun, E. V. Gorbar, and V. P. Gusynin, Phys. Rev. B **81**, 075429 (2010).
- [27] J. Sabio, F. Sols, and F. Guinea, Phys. Rev. B **82**, 121413 (2010).
- [28] J.-R. Wang and G.-Z. Liu, New J. Phys. **14**, 043036 (2012).
- [29] C. Popovici, C. S. Fischer, and L. von Smekal, Phys. Rev. B **88**, 205429 (2013).
- [30] J. Gonzalez, Phys. Rev. B **92**, 125115 (2015).
- [31] M. E. Carrington, C. S. Fischer, L. von Smekal, and M. H. Thoma, Phys. Rev. B **94**, 125102 (2016).
- [32] M. E. Carrington, C. S. Fischer, L. von Smekal, and M. H. Thoma, Phys. Rev. B **97**, 115411 (2018).
- [33] H.-X. Xiao, J.-R. Wang, H.-T. Feng, P.-L. Yin, and H.-S. Zong, Phys. Rev. B **96**, 155114 (2017).
- [34] O. V. Gamayun, E. V. Gorbar, and V. P. Gusynin, Phys. Rev. B **80**, 165429 (2009).
- [35] J. E. Drut and T. A. Lähde, Phys. Rev. Lett. **102**, 026802 (2009).
- [36] J. E. Drut and T. A. Lähde, Phys. Rev. B **79**, 165425 (2009).
- [37] J. E. Drut and T. A. Lähde, Phys. Rev. B **79**, 241405(R) (2009).
- [38] W. Armour, S. Hands, and C. Strouthos, Phys. Rev. B **81**, 125105 (2010).
- [39] W. Armour, S. Hands, and C. Strouthos, Phys. Rev. B **84**, 075123 (2011).
- [40] P. V. Buividovich and M. I. Polikarpov, Phys. Rev. B **86**, 245117 (2012).
- [41] M. V. Ulybyshev, P. V. Buividovich, M. I. Katsnelson, and M. I. Polikarpov, Phys. Rev. Lett. **111**, 056801 (2013).
- [42] D. Smith and L. von Smekal, Phys. Rev. B **89**, 195429 (2014).
- [43] I. S. Tupitsyn and N. V. Prokof'ev, Phys. Rev. Lett. **118**, 026403 (2017).
- [44] F. de Juan and H. A. Fertig, Solid State Commun. **152**, 1460 (2012).
- [45] A. V. Kotikov and S. Teber, Phys. Rev. D **94**, 114010 (2016).
- [46] T. O. Wehling, E. Sasioglu, C. Friedrich, A. I. Lichtenstein, M. I. Katsnelson, and S. Blügel, Phys. Rev. Lett. **106**, 236805 (2011).
- [47] J. A. Gracey, Phys. Rev. D **97**, 105009 (2018).
- [48] N. Dorey and R. D. Kenway, Nucl. Phys. B **333**, 419 (1990).
- [49] K. Kaveh and I. F. Herbut, Phys. Rev. B **71**, 184519 (2005).
- [50] I. F. Herbut, V. Juričić, and B. Roy, Phys. Rev. B **80**, 075432 (2009).
- [51] C. D. Roberts and A. G. Williams, Prog. Part. Nucl. Phys. **33**, 477 (1994).
- [52] J. S. Ball and T. W. Chiu, Phys. Rev. D **22**, 2542 (1980).
- [53] A. S. Mayorov, D. C. Elias, I. S. Mukhin, S. V. Morozov, L. A. Ponomarenko, K. S. Novoselov, A. K. Geim, and R. V. Gorbachev, Nano. Lett. **12**, 4629 (2012).